Search for cosmic neutrinos with ANTARES

Bogazzi, C.

2. Models of astrophysical neutrino emission from Galactic sources

It doesn't matter how beautiful your theory is, it doesn't matter how smart you are. If it doesn't agree with experiment, it's wrong.

Richard P. Feynman

In Chapter 1 we presented potential sources of neutrinos. Here we will focus on Galactic objects and in particular on supernova remnants (SNRs) which are thought to produce the Galactic cosmic rays. In the following sections the sources shown in Figure 1.8 together with theoretical models for neutrino emission from them are discussed. First, a small review of the TeV gamma-ray astronomy is presented to elaborate on the strong connection between the emission of TeV gamma-rays and neutrinos.

2.1. Intermezzo: gamma-ray astronomy

Gamma-ray astronomy covers a very large energy range, namely from low (< 30 MeV) to high (100 MeV - to 50 GeV) and very high (50 GeV - 100 TeV) energies. Due to the opacity of the Earth's atmosphere, the low energy gamma-rays are detected with spaced-based experiments. Unfortunately, satellites can host only relatively small detectors (effective area $\leq 1\ \mathrm{m}^2$). Currently, two gamma-ray satellites are operating: AGILE [70] and Fermi-LAT [40]. The latest catalog of GeV gamma-rays sources released by the Fermi-LAT collaboration contains 1873 sources [71]. Many of these source are not associated with any counterpart in visible light.

At TeV energies, gamma-rays are detected by ground-based imaging atmospheric Cherenkov telescopes (IACTs). IACTs detect the Cherenkov light emitted by charged particles in electromagnetic air showers created by the primary gamma-rays hitting the atmosphere. The three main IACTs are H.E.S.S., MAGIC and VERITAS.

There are about 80 known TeV sources within our Galaxy. Most of them were discovered during the H.E.S.S. survey of the inner Galaxy [72].

2.1.1. Gamma-ray production

In general the light emitted by celestial objects can be divided into two main categories, namely thermal and non-thermal radiation. Thermal radiation is produced by the thermal motion of charged particles in matter. All matter with a temperature above the absolute

zero emits thermal radiation. The most important processes which produce non-thermal radiation are:

- **Synchrotron radiation.** The emission of radio or x-ray photons from electrons moving in a magnetic field.
- **Inverse Compton (IC).** Low energy photons are scattered by relativistic electrons to higher energies.
- **Neutral pion decay**. π^0 mesons produced in p-γ or p-p interactions decay into photons. The π^0 lifetime is $\tau \sim 10^{-16}$ (see Equations 1.14,1.12 for p-p and p-γ interactions and 1.16 for pions decay). The energy of each photon is $m_{\pi^0}c^2/2 = 67.5$ MeV in the rest frame of the π^0.

The first two processes are purely leptonic, i.e. accelerated electrons are responsible for the gamma-ray emission. Hadronic processes such as π^0 production can also be responsible for the VHE photon emission and are associated with the production of neutrinos due to the charged pions decay.

Figure 2.1 illustrates the predicted Spectral Energy Distribution (SED) for the three processes. Two pronounced humps are visible. The first one at X-ray energies (keV), the second one around a few TeV. Synchrotron radiation is responsible for the low-energy hump. The spectrum due to synchrotron radiation follows a power-law function of which the spectral index depends on the energy spectrum of the parent electrons. The high-energy part of the SED is due to (a combination of) IC scattering and π^0 decay. In many leptonic models, the photons produced by synchrotron radiation are the seed photons for the IC process. This is known as self-synchrotron Compton (SSC) emission scenario. The simplest SSC models involve a single population of relativistic electrons emitting synchrotron radiation in radio and X-ray energies and IC photons from X-rays to gamma-rays. Assuming an electron spectrum proportional to $E^{-\alpha}$, in the non-relativistic regime (Thomson limit, $E_e E_\gamma \ll m_e^2 c^2$) the IC scattering produces in the TeV region a flatter spectrum with spectral index $(\alpha+1)/2$ [73]. In the ultrarelativistic domain (Klein-Nishina limit, $E_e E_\gamma \gg m_e^2 c^2$) the spectrum is steeper with index $\alpha + 1$.

The π^0 decay spectrum, dN_γ/dE_γ, is symmetric around 67.5 MeV in a log-log representation (pion-bump). In the SED distribution, $E_\gamma^2 dN_\gamma/dE_\gamma$, it rises steeply below $\sim$ 200 MeV and approximately follows the energy distribution of the parent protons up to energies greater than a few TeV with the same spectral index. The difference in the normalisation between the π^0 decay and the IC scattering spectrum is mainly due to source properties such as, for SNRs, the magnetic field and the proton density, $n_{\rm H}$. Ellison et al. [74] showed that the π^0 decay flux increases more rapidly with $n_{\rm H}$ than the IC flux. More quantitatively, at 1 TeV the ratio between the number of photons due to pion decay and the number of IC photons, $n_\gamma^\pi/n_\gamma^{\rm IC}$, is 0.01 for $n_{\rm H} = 0.01$ cm^{-3} and 0.65 for $n_{\rm H} = 1$ cm^{-3}. A proton density greater than 1 cm^{-3} yields a ratio $(n_\gamma^\pi/n_\gamma^{\rm IC})_{\rm 1TeV} > 1$.

Figure 1.10 shows the energy spectrum for the two SNR which were identified as sources of cosmic rays by the FERMI-LAT collaboration. The GeV gamma-ray data are well fitted by an hadronic model while the leptonic models do not match the data. In the leptonic models discussed in the paper the values of the local magnetic field and the ambient gas

density are chosen to fit both the synchrotron radio and the gamma-ray flux[1]. The low-energy breaks found in data for energies below 200 MeV is not explained by these models, even when assuming an additional low-energy break in the electron spectra to make the gamma-ray spectra below 200 MeV as hard as possible.

The discovery of TeV gamma-ray emitters represents the first step towards the identification of cosmic ray sources (provided that is possible to disentangle the hadronic contribution from the IC). Multi-wavelength observations of the source, from the radio energies to the TeV domain, can contribute to the identification.

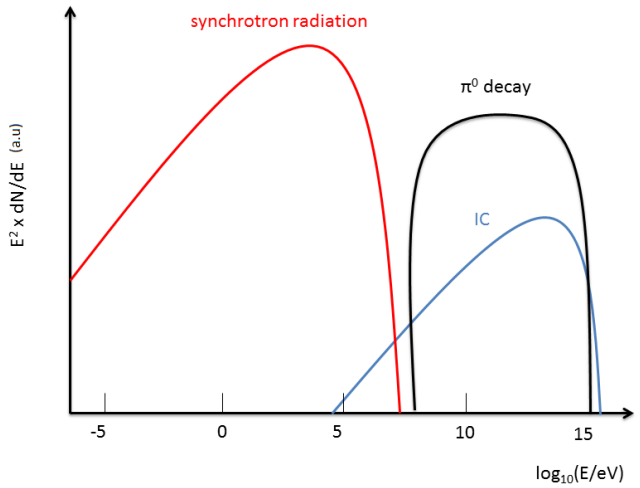

Figure 2.1.: Spectral energy distribution for synchrotron radiation, inverse compton and π^0 decay.

In the next sections we will focus on three Galactic candidate sources of neutrinos. For each of them three neutrino emission models will be discussed. Flux parameters and event rates are reported in Table 2.1.

2.2. RX J1713.7-3946

RX J1713.7-3946 (also known as G347.3-0.5) is a supernova remnant associated with a core collapse supernova which exploded in the constellation of Scorpius in 393 A.D. [75]. It is 1 kpc far from the Earth [76] and has an angular diameter of roughly 1° with a shell of ~ 20 pc size. It was first discovered in the X-rays by ROSAT [77]. Its X-ray spectrum

[1] Due to bremsstrahlung.

is completely dominated by synchrotron emission [78] with very faint thermal X-ray and radio emission.

RX J1713.7-3946 is better known for being the first SNR for which TeV gamma-rays were clearly detected [79]. A detailed campaign from H.E.S.S. revealed indeed a bright TeV gamma-ray emitter with an energy spectrum measured up to 10 TeV and well described by a power law with spectral index of 2.2 [38]. The gamma-ray morphology of RX J1713.7-3946 is shown in Figure 2.2

The main open question regarding RX J1713.7-3946 is the origin of its TeV gamma-rays. A hadronic mechanism would reveal a connection between TeV gamma-ray photons and accelerated protons via the decay of pions, while a leptonic mechanism would suggest that the TeV emission is caused by inverse Compton scattering of the photon fields near the remnant by the same relativistic electrons that are responsible of the X-ray emission. In this regard, the recent results published in 2011 by the Fermi-LAT collaboration [81] are of particular importance since they collected data in the energy range (500 MeV to 400 GeV) which closes the gap between X-ray satellites measurements and TeV gamma-ray telescopes. Figure 2.3 (top) shows the energy spectrum measured by Fermi-LAT at low energies and H.E.S.S. at high energies. The hard spectrum in the energy range 1-100 GeV agrees with leptonic models describing the gamma-ray emission as consequence of IC scattering (see also Figure 2.1). Pure hadronic models seems to be disfavored by these measurements as can be inferred by Figure 2.3 (bottom). In particular, the lack of thermal X-ray emission yields a small proton density in the SNR since the main sources responsible for the heating of the electrons are Coulomb collisions between electrons and protons [74]. However, the good agreement between Fermi-LAT data and leptonic processes models does not mean that protons are not accelerated in this SNR and an hybrid scenario (leptonic and hadronic) [82] can not be ruled out. The proton spectral index that can be inferred from the LAT data is $\alpha =\sim 1.5$ a value which is as small as the asymptotic limit of $\alpha = 1.5$ predicted for extremely efficient CRs acceleration [83]. Recently Inoue et al. [84] showed that the X-ray thermal emission could suppressed by molecular clouds which stall the accelerated shock wave. The interaction between the accelerated CR protons and the protons of the clouds could produce neutral pions. The derived photon index of the hadronic gamma-rays is consistent with the FERMI-LAT observations.

2.2.1. Neutrino emission from RX J1713.7-3946

In the last decade many theoretical models to describe neutrino emission from RX J1713.7-3946 have been developed. We consider three recent models proposed after the latest H.E.S.S. measurements. In these models, a similar neutrino spectrum which follows a power-law distribution with exponential cut-off is obtained:

$$\frac{dN_\nu}{dE_\nu} = k_\nu (\frac{E_\nu}{1\mathrm{TeV}})^{-\Gamma_\nu} \exp(-\sqrt{(}E_\nu/E_{c,\nu})). \tag{2.1}$$

The values of the flux normalisation, k_ν, the spectral index, Γ and the cut-off energy $E_{c,\nu}$ for each of these models are reported in Table 2.1.

- **Kistler and Beacom (2006).** The authors of [50] present a model based on the measured parameters of the gamma-ray spectrum for various Galactic sources. The

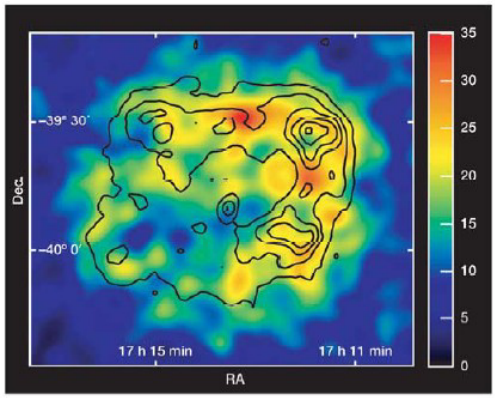

Figure 2.2.: Gamma-ray image of the SNR RX J1713.7-3946. Figure taken from [38].

following assumptions were made:

1. The gamma-ray and the neutrino flux share the same spectral index Γ (2.2 for RX J1713.7-3946 as reported in [38]).
2. In p-p interactions, for equal pion multiplicities each photon from π^0 decay corresponds to a neutrino from $\pi^{\pm}$ decay. The energy of these neutrinos is roughly half of the photon energy. The resulting neutrino spectrum is then shifted, relative to the gamma-ray spectrum and

$$\frac{dN_\nu}{dE_\nu} = k_\nu E_\nu^{-\Gamma} = (\frac{1}{2})^{\Gamma-1} k_\gamma E_\nu^{-\Gamma} \tag{2.2}$$

   thus, the relation between the gamma and neutrino flux normalisation is given by:

$$k_\nu = k_\gamma (\frac{1}{2})^{\Gamma-1}, \tag{2.3}$$

   with $k_\gamma = 15 \times 10^{-12} \mathrm{TeV}^{-1} \mathrm{cm}^{-2} \mathrm{s}^{-1}$ (as reported in [38]).
3. The neutrinos are assumed to cut-off at half the observed gamma cut-off, i.e. $E_{c,\nu} = 0.5 \cdot E_{c,\gamma}$ (for RX J1713.7-3946 $E_{c,\nu} = 50$ TeV).

- **Kappes et al. (2007).** A neutrino emission model which can be applied to most of the known Galactic sources is proposed in [95]. Parametrisations of simulated energy spectra of pions and secondary particles produced in inelastic proton- proton collisions are presented in [96]. These parametrisations are used to calculate the relationship between gamma-ray and neutrino spectra. The primary proton spectrum is given by a power law with spectral index Γ and exponential cut-off energy $E_{c,p}$:

$$\frac{dN_p}{dE_p} = k_p (\frac{E_p}{1\mathrm{TeV}})^{-\Gamma_p} \exp(-\frac{E_p}{E_{c,p}}). \tag{2.4}$$

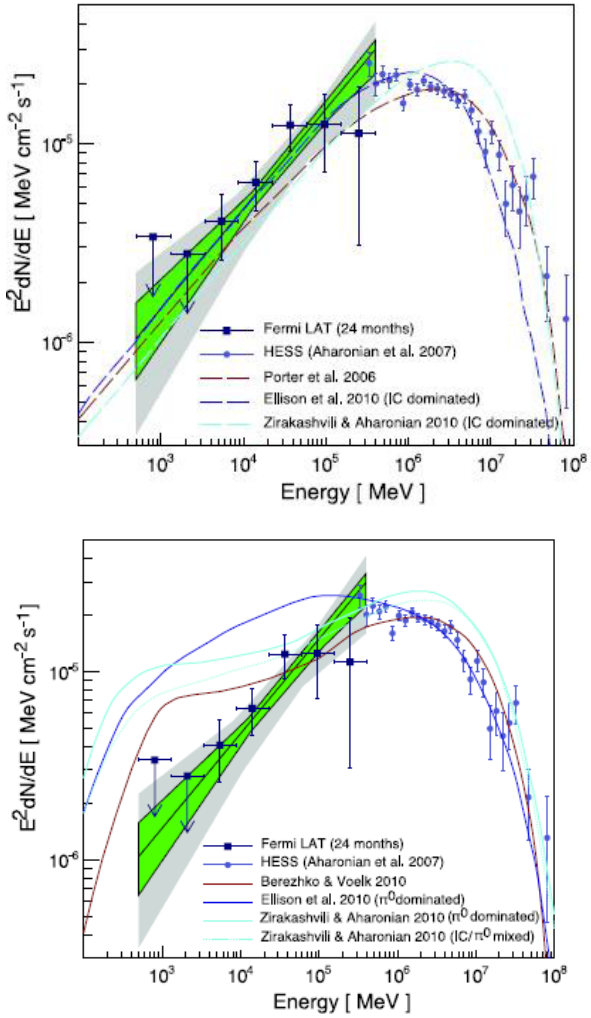

Figure 2.3.: Energy spectrum of RX J1713.7-3946 with data from Fermi-LAT and H.E.S.S. [38]. The top plot features predictions where the photons are produced via the leptonic mechanism. The bottom plot shows several models where the photons are generated via the hadronic mechanism. Fermi-LAT data agrees with emission scenarios in which the dominant source of emission is IC scattering. Both figures are taken from [81].

The resulting γ-ray and neutrino spectra follows the function given in Equation 2.1 with:

$$\begin{aligned} k_\nu &\simeq (0.71 - 0.16\Gamma_p)k_\gamma \\ \Gamma_\nu &\simeq \Gamma_\nu \simeq \alpha - 0.1 \\ E_{c,\nu} &\simeq 0.59 E_{c,\gamma} \simeq E_{c,p}/40 \end{aligned} \tag{2.5}$$

For RX J1713.7-3946 the flux normalisation $k_\nu = 15 \times 10^{-12}\mathrm{TeV}^{-1}\mathrm{cm}^{-2}\mathrm{s}^{-1}$, the spectral index $\Gamma_\nu = 1.72$ and the energy cut-off $E_{c,\nu} = 1.35\ \mathrm{TeV}$.

Several assumptions are made in these calculations. Among them we emphasize the following:

1. The radiation and the matter densities of the source are sufficiently low for the photons to escape without interacting. This also means that the charged pions and the muons decay before interacting (matter density low) and that p-γ interactions are neglected (radiation density low).
2. Muons decay without losing a significant fraction of the energy. This is possible only for low magnetic fields (B $\sim$ few μG).
3. A total neutrino mixing occurs $(\nu_e : \nu_\mu : \nu_\tau) = (1{:}1{:}1)$

For RX J1713.7-3946 all these assumptions seem reasonable.

- **Morlino et al. (2009).** Unlike the previous models, the one described in [97] is based on a non linear diffuse shock acceleration (NLDSA) approach. The idea behind the NLDSA theory is to overcome one of the main problems of the so-called *test particle* approximation of particle acceleration in collisionless shocks. In the first order Fermi mechanism, a fraction of the kinetic energy of the moving stream has to be transferred to the accelerated particles, a clear contradiction of the assumption that the accelerated particles are test particles [98]. The fact that the spectrum is described by a power law is a consequence of this assumption. In NLDSA theory a dynamical backreaction of the accelerated particles on the shock is assumed: the pressure of the accelerated particles affects the shock dynamics [97, 99]. This leads to a shape of the spectrum of the accelerated particles which is not a simple power law but rather a more complicated one that can be as hard as $p^{-3.2}$ for high momenta p of the accelerated particle.

  The neutrino flux derived has $k_\nu = 3.01 \times 10^{-14}\mathrm{GeV}^{-1}\mathrm{cm}^{-2}\mathrm{s}^{-1}$, $\Gamma_\nu = 1.78$ and $E_{c,\nu} = 2.6\ \mathrm{TeV}$.

In Figure 2.4 the predicted neutrino fluxes for the three models discussed are shown. Despite the different assumptions made, these models produce similar fluxes. In particular, the proposed spectral index and cut-off energy in the models from Kappes et al. and Morlino et al. agree, but the flux normalisation differs. The predicted number of signal events for this analysis which is reported in Table 2.1 is quite low (less than one event is expected).

2.3. Vela X

The Vela supernova remnant is the closest SNR which contains a pulsar, PSR B0833-45. It is located at a distance of roughly 290 pc [85]. The pulsar has a period of 89.3 ms and a period derivative of 1.25 $\times$ 10^{-13} s s^{-1}, Its age is 11 kyr[2]. Radio and X-ray

[2]Assuming a braking index $\mathrm{n} = 3$, i.e. the magnetic dipole radiation is responsible for the spin-down of the pulsar

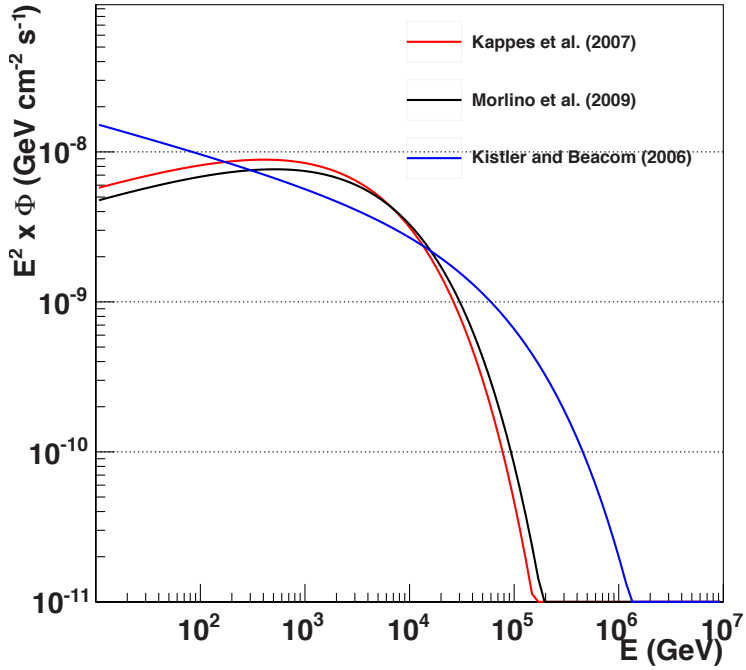

Figure 2.4.: Estimated neutrino flux from RX J1713.7-3946 as a function of the neutrino energy for the three models considered in the text: blue line for Kistler and Beacom (2006) [50], red line for Kappes et al. [95] (2007) and black line for Morlino et al. (2009) [97].

observations showed the presence of a large diffuse emission surrounding the pulsar. These radio observations established that within the 8 degrees diameter of Vela SNR there are three distinct regions of bright diffuse emission. The most intense of these regions is Vela X. It is generally believed that Vela X is a pulsar wind nebula (PWN) formed by material ejected from PSR B0833-45.

Very high-energy gamma-rays were observed by H.E.S.S. in 2006 and 2012 [42, 86]. It should be noted that the latest data yield an integral flux which is a factor 1.6 higher than previously reported. A comparison between the differential gamma-ray spectra is shown in Figure 2.5 (left) together with the source morphology (right).

The wide-band emission from Vela X is well explained by a two-zone leptonic model [87]: the gamma-ray emission is described through IC by a first population of electrons accelerated in the vicinity of the Vela pulsar. These electrons are also responsible of the synchrotron emission in X-rays. A second population of electrons with lower energies and more extended spatial distribution give rise to the radio emission.

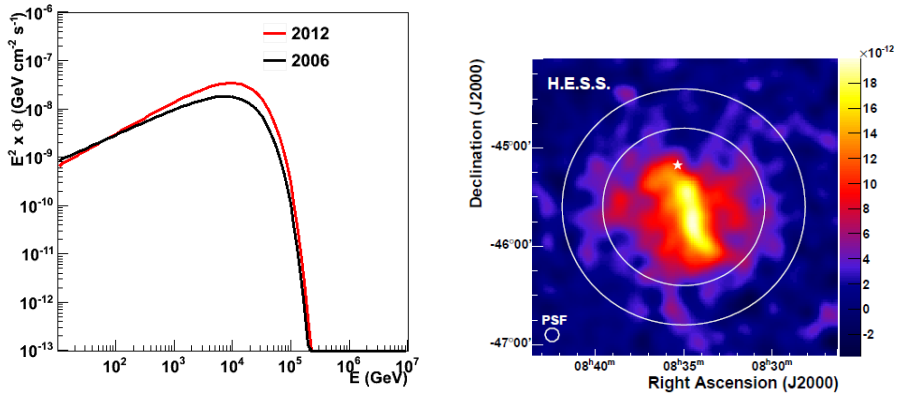

Figure 2.5.: Left: exponential cut-off power law functions which give the best fit results of the differential gamma-ray spectrum in the TeV energy range for the PWN Vela X. The black line shows the function used to fit the H.E.S.S. data from 2006. The red line corresponds to the function which fitted the H.E.S.S. data from 2012. Right: TeV image of Vela X. Figure taken from [42].

2.3.1. Neutrino emission from Vela X

Being one of the brightest Galactic sources, Vela X is an interesting candidate neutrino source. Several theoretical models of neutrino emission have been developed in the last decade. We discuss only on three of them. The neutrino flux proposed is described by a power-law function with exponential cut-off as in Equation 2.1.

- **Kistler and Beacom (2006).** The model presented in [50] was already discussed in Section 2.2.1. It also applied to Vela X. The values of the flux parameters are now $k_\nu = 6.6 \times 10^{-12}\mathrm{TeV}^{-1}\mathrm{cm}^{-2}\mathrm{s}^{-1}$, $\Gamma_\nu = 1.45$ and $E_{c,\nu} = 7\,\mathrm{TeV}$.

- **Kappes et al. (2007).** The spectrum parameters derived by Kappes et al. for Vela X are $11.75 \times 10^{-12}\ \mathrm{TeV}^{-1}\mathrm{cm}^{-2}\mathrm{s}^{-1}$, 0.98 and 0.84 $0.84\,\mathrm{TeV}$ for k_ν, Γ_ν and $E_{c,\nu}$ respectively.

- **Villante & Vissani (2008).** As last model for neutrino emission from Vela X, we consider the one described in [100] which does not need a preliminary parametrisation of the gamma-ray observations but uses directly the gamma-ray data as input. Neutrinos and hadronic gamma-rays are considered to be linked by a linear relation:

$$\Phi_\nu(E_\nu) = 0.380\Phi_\gamma(\frac{E_\gamma}{1-r_\pi}) + 0.013\Phi_\gamma(\frac{E_\gamma}{1-r_K}) + \int_0^1 \frac{dx}{x} K_\mu \Phi_\gamma(\frac{E_\gamma}{x}), \qquad (2.6)$$

  where the first and the second terms take into account neutrinos produced in pions and kaons respectively with $r_{\pi,K} = (m_\mu/m_{\pi,K})^2$. The kernel K_μ describes neutrinos

produced by muon decay and can be expressed as:

$$K_\mu(x) = \begin{cases} x^2(15.34 - 28.93x) & 0 < x < r_K \\ 0.0165 + 0.1193x + 3.747x^2 - 3.981x^3 & r_K < x < r_\pi \\ (1-x)^2(-0.6698 + 6.588x) & r_\pi < x < 1 \end{cases} \quad (2.7)$$

Similar equations describe the antineutrino emission. The calculated flux can then be fitted by power law function with exponential cut-off with $k_\nu = 0.94 \times 10^{-14} \mathrm{TeV}^{-1}\mathrm{cm}^{-2}\mathrm{s}^{-1}$, $\Gamma_\nu = 1.32$ and $E_{c,\nu} = 8\,\mathrm{TeV}$.

The predicted neutrino fluxes from the three models described above are shown in Figure 2.6. Villante and Vissani propose a neutrino flux which is well above the prediction from Kistler and Beacom and Kappes et al. This is due to the different gamma-ray data considered. The results from Villante and Vissani were derived for the latest H.E.S.S. results while the other two predictions are based on the H.E.S.S. data from 2006.

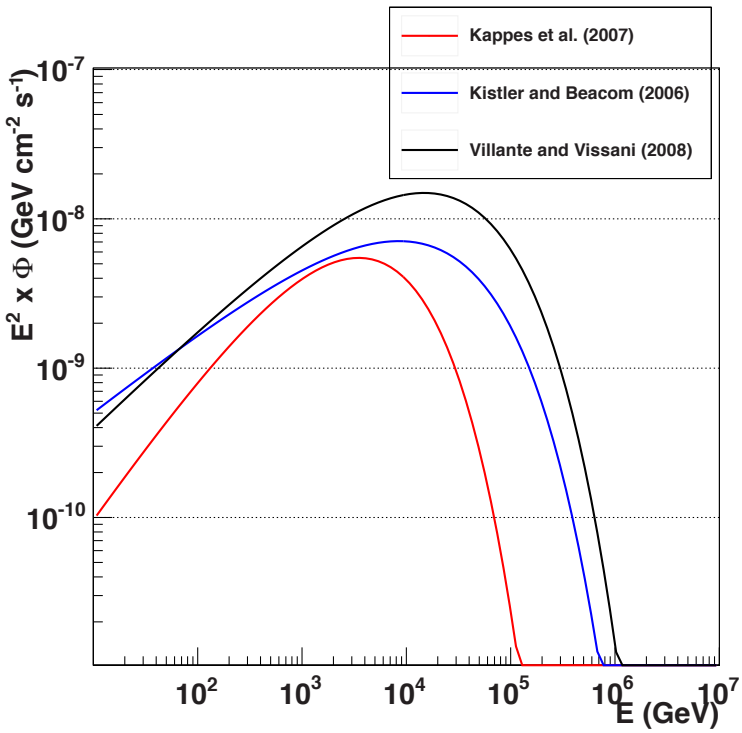

Figure 2.6.: Estimated neutrino flux from Vela X as a function of the neutrino energy for the three models considered in the text: blue line for Kistler and Beacom (2006) [50], red line for Kappes et al. [95] (2007) and black line for Villante and Vissani (2008) [100].

The expected number of signal events from Vela X assuming each one of the models is reported in Table 2.1. As for RX J1713.7-3946, also for Vela X less than one event is

expected for this analysis.

2.4. Crab

The Crab Nebula is a supernova remnant with a central pulsar located about 2 kpc from Earth. The associated SN explosion was observed in 1054 A.D. by Arabic, Chinese, Indian and Japanese astronomers. The Crab Nebula was discovered in 1731 by the English astronomer John Bevis. The central pulsar PSR B0531+21, the most energetic pulsar in the Galaxy, has a spin-down power of $4.6 \times 10^{38}\,\mathrm{erg\ s^{-1}}$.

The Crab Nebula was discovered at TeV energies in 1989 [88] by the Whipple 10 m telescope, followed by several others experiments [89, 90, 91]. The TeV gamma-ray flux from the Crab Nebula is the highest. Recent observations from the AGILE satellite [92] and FERMI-LAT [93] have discovered strong gamma-ray flares (up to 10 GeV), raising a new interest for this source.

The SED of the non-thermal emission shows two components. The low energy component can be explained by synchrotron radiation of high-energy electrons travelling through the magnetic fields of the nebula. The same electron population is responsible for the high-energy component attributed to IC scattering of photons by these electrons.

2.4.1. Neutrino emission from Crab Nebula

Although the Crab Nebula is visible at the ANTARES site for roughly 40% of the day, we report and discuss neutrino emission from this PWN keeping in mind that despite a low visibility the Crab Nebula is the brightest Galactic source. Most of the energy of the pulsar which powers the Crab Nebula is carried by a magnetised wind of relativistic plasma. The composition of this plasma is still not known. The majority of the models predicting neutrino emission from the Crab consider a plasma composed by a mixture of $e^{\pm}$, responsible of synchrotron radiation and IC scattering, and protons or ions which generate charged mesons via p-p or p-γ interactions. Indeed, a common assumption shared by these models is that a significant fraction of the rotational energy lost by the pulsar is transferred to relativistic nuclei in the nebula, which can interact with the local matter and produce CRs and neutrinos via pion decay.

An interesting model of neutrino emission is described in [101] (2005). In this, positive ions can be accelerated up to 1 PeV on the surface of young rotating neutron stars ($\leq 10^5$ yrs). A beam of muon neutrinos is produced by high-energy protons interacting with surface X-ray photons when the photomeson production resonance is reached. However, this model has been excluded at more than 90% CL by the recent IceCube point source analysis with 40 strings [59].

We now discuss three models which predict a neutrino flux parametrised by a power-law function with exponential cut-off.

- **Amato et al. (2003)**. This model [102] investigates the transfer of rotational energy lost by the pulsar to the relativistic nuclei in the pulsar wind, which is considered to be composed of these heavy ions and a denser plasma of electron-positrons pairs.

Alfvén cyclotron waves are generated by the nuclei when they meet the pulsar wind shock [103]. These Alfvén waves will resonantly scatter off positrons and electrons accelerating them [31], which are responsible for the synchrotron emission. After crossing the shock, the relativistic nuclei drift towards the outer part of the nebula. They may interact with the plerion radiation field and the ejected material to create pions which decay to neutrinos. The pion differential spectra for the p-p scattering is described as:

$$\frac{dN_\pi}{dE_\pi dt} = K_\pi E_\pi^{-1} g_\pi(E_\pi/E_p), \tag{2.8}$$

where E_p is the energy of the primary proton and the function g is parametrised as follows:

$$g_\pi(x) = (1-x)^{3.5} + \frac{e^{-18x}}{1.34}. \tag{2.9}$$

The variable K_π is related to the pulsar spin-down luminosity and to the probability for a relativistic proton to create a pion before losing energy.

The differential neutrino flux is given by:

$$\frac{dN_\nu}{dE_\nu dt} \simeq 4(1+f^\nu[3E_\nu])f^\mu[4E_\nu]\frac{dN_{\pi^\pm}}{dE_{\pi^\pm}dt}|_{E_{\pi^\pm}=4E_\nu} \tag{2.10}$$

where $f^\mu = \min[1, \mathrm{t}^\pi_{\mathrm{losses}}/\mathrm{t}^\pi_{\mathrm{decay}}]$ and $f^\nu = \min[1, \mathrm{t}^\mu_{\mathrm{losses}}/\mathrm{t}^\mu_{\mathrm{decay}}]$ take into account the energy loss of pions and muons before decaying and are derived from simulations for different Lorentz factors of the pulsar wind. The derived neutrino flux can be approximated by the function in Equation 2.1. The calculated parameters for the optimistic case with a Lorentz factor $\Gamma = 10^7$ are $k_\nu = 3.7 \times 10^{-14}\mathrm{TeV}^{-1}\mathrm{cm}^{-2}\mathrm{s}^{-1}$, $\Gamma_\nu = 1.08$ and $E_{c,\nu} = 6.47 \times 10^2 \mathrm{TeV}$.

Although the predicted flux was excluded at 90% CL by IceCube [59], it is still interesting to investigate the response of the detector assuming this model for a source like the Crab Nebula with a low visibility.

- **Kistler and Beacom (2006).** As for RX J1713.7-39 and Velax, also for the Crab Nebula we report the neutrino flux predicted in [50]. The values considered for k_ν, Γ_ν and $E_{c,\nu}$ are respectively $11 \times 10^{-12}\mathrm{TeV}^{-1}\mathrm{cm}^{-2}\mathrm{s}^{-1}$, 2.57 and $50\ \mathrm{TeV}$.

- **Kappes et al. (2007).** The model described in [95] is also applied to the case of the Crab Nebula. The values of the flux normalisation, spectral index and cut-off energy are changed accordingly and are:

$$\begin{cases} k_\nu = 22.3 \times 10^{-15}\mathrm{GeV}^{-1}\mathrm{cm}^{-2}\mathrm{s}^{-1} \\ \Gamma_\nu = 2.15 \\ E_{c,\nu} = 1.72\ \mathrm{TeV} \end{cases} \tag{2.11}$$

Figure 2.7 shows the expected neutrino fluxes for these three models and Table 2.1 summarizes them. Amato et al. predict a cut-off energy roughly one order of magnitude higher than the other two models. The spectral index also differs. This is because Kistler

and Beacom and Kappes et al. based their predictions on the H.E.S.S. data which were not published yet when Amato et al. proposed their model.

The expected number of events for this analysis is significantly smaller than for the other sources and models considered. This is mainly due to the location of the Crab Nebula which is visible only for a fraction of the day of 40%.

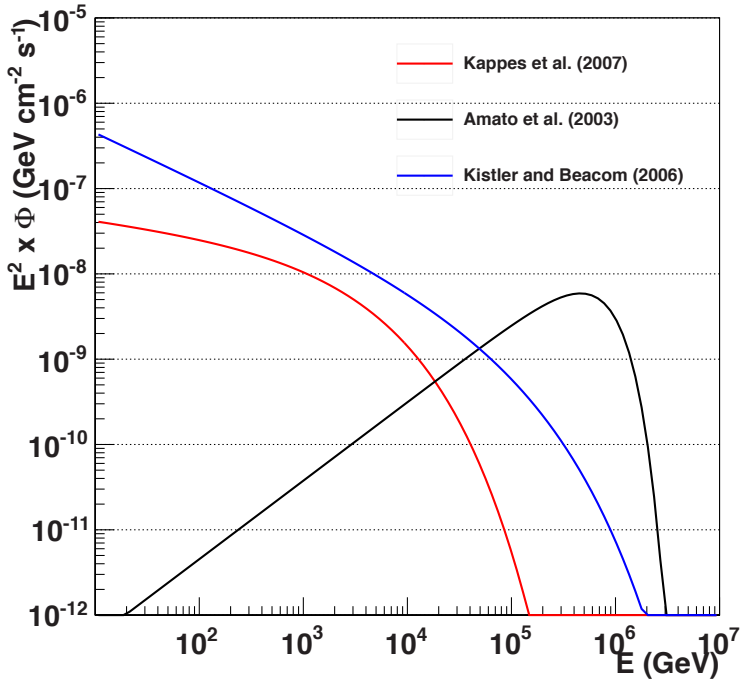

Figure 2.7.: Neutrino fluxes from the Crab Nebula as a function of the neutrino energy: blue line for Kistler and Beacom (2006) [50], red line for Kappes et al. [95] (2007) and black line for Amato et al. (2003) [102].

Source	Models	$k_\nu[\mathrm{GeV}^{-1}\mathrm{cm}^{-2}\mathrm{s}^{-1}]$	Γ_ν	$E_{c,\nu}[\mathrm{GeV}]$	$\hat{N}_{\mathrm{sig}}$
RX J1713.7-3946	Kistler & Beacom	15×10^{-15}	2.19	5×10^4	0.12
	Kappes et al.	16.8×10^{-15}	1.78	2.1×10^3	0.13
	Morlino et al.	3.01×10^{-14}	1.78	2.6×10^3	0.11
Vela X	Kistler & Beacom	6.58×10^{-15}	1.45	7×10^3	0.15
	Kappes et al.	11.75×10^{-15}	0.98	840	0.20
	Villante & Vissani	9.3×10^{-15}	1.32	8×10^3	0.60
Crab	Kistler & Beacom	11.1×10^{-15}	2.57	5×10^4	0.09
	Kappes et al.	2.23×10^{-14}	2.15	1.72×10^4	0.05
	Amato et al.	3.76×10^{-17}	1.08	6.47×10^5	0.09

Table 2.1.: Flux normalisation (third column), spectral-index (fourth column) and cut-off energy (fift column) assuming a neutrino flux parametrised by a power-law function with exponential cut-off for each source and model considered. The last column shows the expected number of events that would be selected by ANTARES using the data set 2007-2010 and applying the same cuts of the analysis described in this thesis.